Published in final edited form as:
J Am Chem Soc. 1998 September 23; 120(37): 9605–9613.

Activation Energies for Dissociation of Double Strand Oligonucleotide Anions: Evidence for Watson–Crick Base Pairing in Vacuo

Paul D. Schnier, **John S. Klassen**, **Eric F. Strittmatter**, and **Evan R. Williams***
Contribution from the Department of Chemistry, University of California, Berkeley, California 94720

Abstract

The dissociation kinetics of a series of complementary and noncomplementary DNA duplexes, $(TGCA)_2^{3-}$, $(CCGG)_2^{3-}$, $(AATTAAT)_2^{3-}$, $(CCGGCCG)_2^{3-}$, $A_7{\cdot}T_7^{3-}$, $A_7{\cdot}A_7^{3-}$, $T_7{\cdot}T_7^{3-}$, and $A_7{\cdot}C_7^{3-}$ were investigated using blackbody infrared radiative dissociation in a Fourier transform mass spectrometer. From the temperature dependence of the unimolecular dissociation rate constants, Arrhenius activation parameters in the zero-pressure limit are obtained. Activation energies range from 1.2 to 1.7 eV, and preexponential factors range from 10^{13} to 10^{19} s^{-1}. Dissociation of the duplexes results in cleavage of the noncovalent bonds and/or cleavage of covalent bonds leading to loss of a neutral nucleobase followed by backbone cleavage producing sequence-specific (**a** – base) and **w** ions. Four pieces of evidence are presented which indicate that Watson–Crick (WC) base pairing is preserved in complementary DNA duplexes in the gas phase: i. the activation energy for dissociation of the complementary dimer, $A_7{\cdot}T_7^{3-}$, to the single strands is significantly higher than that for the related noncomplementary $A_7{\cdot}A_7^{3-}$ and $T_7{\cdot}T_7^{3-}$ dimers, indicating a stronger interaction between strands with a specific base sequence, ii. extensive loss of neutral adenine occurs for $A_7{\cdot}A_7^{3-}$ and $A_7{\cdot}C_7^{3-}$ but not for $A_7{\cdot}T_7^{3-}$ consistent with this process being shut down by WC hydrogen bonding, iii. a correlation is observed between the measured activation energy for dissociation to single strands and the dimerization enthalpy ($-\Delta H_d$) in solution, and iv. molecular dynamics carried out at 300 and 400 K indicate that WC base pairing is preserved for $A_7{\cdot}T_7^{3-}$ duplex, although the helical structure is essentially lost. In combination, these results provide strong evidence that WC base pairing can exist in the complete absence of solvent.

Introduction

"Soft" ionization techniques, such as electrospray ionization (ESI)[1] and matrix-assisted laser desorption ionization (MALDI),[2] make possible the formation of intact gas-phase ions from nonvolatile and thermally labile molecules. These methods have transformed mass spectrometry (MS) into a powerful tool for the analysis of large biopolymers including proteins and DNA.[3] Molecular weights can be measured with low part per million mass accuracy even for proteins with molecular weights greater than 100 kDa.[4] Tandem mass spectrometry (MS/MS) has become an important and established method for determining the primary structure of small peptides[5–7] and oligonucleotides.[8–11] An emerging application of MS is the analysis of noncovalent biomolecule complexes in solution.[12–24] The interactions in these complexes are of paramount importance in biological systems as they form the basis for molecular recognition. ESI "gently" transfers ions from solution to the gas phase. In addition, gas-phase ions can be generated from buffered aqueous solutions which simulate in vivo conditions. Numerous non-covalent complexes of biomolecules known to exhibit specificity in solution have been observed in ESI mass spectra, including antibody–antigen,[16] enzyme–substrate,[17] and receptor–ligand[18] complexes, and DNA duplexes.[19–24]

Solvent is generally believed to play a dominant role in the formation and stabilization of specific interactions between biomolecules. Consequently, there is considerable debate regarding the structure of these complexes in the gas phase.[25] A key question that remains unanswered is whether the interactions which lead to specificity in solution can be preserved during the ESI process and the eventual removal of solvent. A number of studies in which the kinetic stabilities of noncovalent complexes in the gas phase have been compared to those in solution have been reported. A correlation has been demonstrated for some heme–protein complexes,[26,27] while no correlation was observed for certain protein–protein and enzyme–inhibitor complexes.[28,29] Clearly, the chemical nature of the interactions will govern the response of the complex to the removal of solvent.

Noncovalent interactions involving DNA and other biopolymers, such as DNA, RNA, and proteins, are essential in a variety of biological processes. In aqueous solutions, complementary strands of DNA can form a stable complex with a helical structure referred to as a double helix. The two strands are held together by hydrogen bonds formed between complementary base pairs, A·T and C·G, which adopt a Watson–Crick (WC) geometry (Scheme 1). Each A·T pair can form two hydrogen bonds, while each C·G pair can form three.

The double helix is also stabilized by base stacking, where adjacent planar bases within a strand stack one on top of each other thereby stabilizing the three-dimensional structure of the duplex. The origin of this interaction has been widely debated but is generally ascribed to a hydrophobic effect as well as dispersion forces between the face of the bases.[30]

DNA duplexes are readily observed in a ESI mass spectra of oligonucleotides under gentle sampling conditions.[19–24] McLafferty and co-workers[22] demonstrated that the base composition of DNA strands can be determined from accurate molecular weight measurements of double-strand DNA ions. Ding and Anderegg[21] reported that the relative abundance of DNA duplex ions in ESI mass spectra qualitatively reflect the abundance of these duplexes in solution. In addition to duplexes, intact DNA quadraplexes,[31] DNA protein complexes,[32] and DNA drug complexes[32–34] have been observed by mass spectrometry.

With blackbody infrared radiative dissociation (BIRD), whereby ions are activated by absorption of blackbody photons, it is possible to measure Arrhenius activation energies (E_a) and entropies ($\Delta S^{\ddagger}$) for dissociation of large biomolecules and complexes in vacuo.[35,36] BIRD has been used to measure Arrhenius parameters for the dissociation of a variety of small ions and clusters,[37–42] peptides,[43,44] and proteins.[27,35,45,46] Here, BIRD is used to provide the first quantitative measurements of gas-phase dissociation activation energies and entropies of anionic oligonucleotide duplexes. These and other data strongly indicate that WC base pairing that exists in solution is preserved in the gas phase.

Experimental Section

All BIRD experiments were performed on a 2.7 T Fourier transform mass spectrometer. Both the instrument and the BIRD experiment are described in detail elsewhere.[44,45] The DNA samples were synthesized by the Center for Biotechnology at Cornell University and desalted using two steps of HPLC. Gas-phase DNA anions were generated by electrospraying ~10^{-4} M solutions of oligonucleotides in 50:50 H_2O/ CH_3CN. Microelectrospray needles were constructed from 1.0 mm o.d. aluminosilicate capillaries which were pulled to a diameter of ~2 μm o.d. at one end using a micropipet puller (Sutter Instruments Inc., Novato, CA). The electric field required to initiate the electrospray was established by applying a voltage of ~−1 kV to a Pt wire inserted into the ESI needle to within 1–2 mm of the tip. The distance between the microspray needle tip and the heated metal capillary of the mass spectrometer was typically ~1 mm. Under normal operating conditions, solution flow rates were ~60–100 nL/min. The electrospray ions were sampled from atmospheric pressure through a 0.50 mm i.d. heated

stainless steel capillary and guided into the magnet via a series of electrostatic lenses. The temperature of the stainless steel capillary was 90 °C; the temperature of the droplets as they pass through the capillary is not known. Lowering the temperature of the capillary results in loss of ion signal. This temperature was selected to be the lowest possible in order to obtain a significant abundance of duplex ions. At higher capillary temperatures, the overall signal increases, but the signal for the duplex decreases.

Ions were collected in the FTMS ion cell for 5–15 s duration. To improve ion trapping efficiency, N_2 was pulsed into the ion cell region at pressures of ~10^{-6} Torr during ion accumulation. Isolation of the desired precursor ions was achieved using both single frequency rf and SWIFT excitation. The temperature of the vacuum chamber, which establishes the blackbody radiation field, was controlled using a heating blanket with a proportional temperature controller (Omega Inc., Stamford, CT, model 4002A) and was monitored using four copper–constantan thermocouples located around the ion cell. The temperature difference between these thermocouples at the highest temperatures used was less than 2 °C.

Mass spectra were acquired using an Odyssey Data System (Finnigan-FTMS, Madison, WI) using a rf sweep (120 V peak-to-peak, 1100 Hz/μs) for ion excitation prior to detection; 128 × 10^3 data points were collected. Dissociation rate constants were obtained by performing a standard unweighted linear least-squares analysis to a plot of ln([M]/ ([M] + ∑[F])) versus reaction delay, where M and F are the precursor and fragment ions, respectively. The signal in FTMS is directly proportional to the charge state and abundance of the ion. Since charge in these reactions is conserved, the precursor and fragment ion abundances are used directly to obtain the dissociation rate constants. The errors in the Arrhenius activation parameters were obtained by calculating the variances and covariances (ANOVA table) of the Arrhenius activation energies (E_a) and frequency factors (A), from the linear regression data. This error analysis assumes that the kinetic data are independent and reflects uncertainties due to random errors. Systematic errors, which could be introduced from nonuniform heating of the vacuum chamber and differences in the detection efficiencies of different mass fragment ions, are not taken into account.

The DNA duplex melting curves, where absorbance (at 260 nm) is plotted versus temperature, were measured with a variable temperature spectrophotometer using a 5 cm cell. The solvent composition is the same as that used for ESI (50:50 H_2O/CH_3CN). The rate of rise in temperature was 0.5 °C/min.

Molecular modeling of $A_7{\cdot}T_7^{3-}$, $A_7{\cdot}A_7^{3-}$ and $T_7{\cdot}T_7^{3-}$ was performed using the Macromodel 6.0 software package (Columbia University, New York, NY) on a Silicon Graphics Impact 10000. The Amber94 force field[47] was used for all the calculations. Šponer and co-workers have demonstrated that binding energies calculated for hydrogen bonded nucleoside dimers with this force field agree, within 1 kcal/mol, with ab initio results obtained at the MP2/6-31G*//6-31G* level.[48] This force field also best reproduces the base stacking stabilization energies.[49] Therefore, this force field should accurately represent base pair hydrogen bonding in these complexes. The starting structures of the three duplexes for the molecular dynamics was a double helix, constructed using the nucleic acid builder in Macromodel. In the case of the two homodimers, the initial structure was optimized prior to dynamics. This energy minimization step had the effect of displacing one of the strands along the axis normal to the bases, such that the bases were slightly offset from one another. The terminal 5′ phosphate hydroxyl group of each strand, as well as the middle phosphate on one of the strands, were chosen as the sites of deprotonation. In the case of the heterodimer, the T_7 strand was chosen to be doubly charged, consistent with the experimental results. For all simulations, a step size of 1.5 fs was used. Structures were stored every 5 and 10 ps for the homodimers and heterodimer, respectively.

Results

Electrospray of Oligonucleotides.

Under gentle sampling conditions, i.e., when ions are not extensively heated by collisions in the electrospray interface, DNA duplexes of complementary strands can be readily observed in ESI mass spectra. Figure 1a shows an ESI mass spectrum obtained from a 1:1 mixture of 10^{-4} M $p(dA)_7$ and $p(dT)_7$ (referred to subsequently as A_7 and T_7) in 50:50 H_2O/CH_3CN. Both the singly and doubly deprotonated monomers are present. The higher abundance of the T_7 monomer relative to A_7 appears to reflect a difference in ionization efficiency, the origin of which is not clear. Also observed is the doubly and triply charged complementary duplex, $T_7{\cdot}A_7^{3-}$, as well as a smaller abundance of the noncomplementary, $A_7{\cdot}A_7^{3-}$ and $T_7{\cdot}T_7^{3-}$, dimers. Annealing this solution has no effect on the abundances of dimer ions observed in the ESI mass spectrum. Noncomplementary strands are known to dimerize at concentrations above 10^{-4} M, although with very weak association constants.[50] Thus, the relative abundances of the complementary versus noncomplementary duplexes in the ESI mass spectrum appear to qualitatively reflect the expected solution-phase specificity of these duplexes.

The presence of duplex in the solution from which these ions are formed was verified by measuring a melting curve. The increased absorption at higher temperature results from the thermal denaturation of the duplex and disruption of base stacking.[30] The curve indicates that the complementary duplex, $T_7{\cdot}A_7$, is stable at temperatures below 30 °C. The higher abundance of the single strand relative to the duplex observed in the ESI spectrum does not agree with the solution composition. This could be due either to thermal dissociation of the duplex in the electrospray droplet as it passes through the heated metal capillary or to dissociation of these duplexes in the gas phase. The former mechanism is more likely since gas-phase dissociation of the duplexes can lead to other fragment ions that are not observed in large abundances in the ESI mass spectra.

In general, the abundances of noncomplementary DNA dimer ions observed in the ESI mass spectra are significantly lower than those of the complementary duplexes as has been reported previously.[21] For example, the abundance of noncomplementary $C_7{\cdot}C_7^{3-}$ formed from a solution containing 10^{-4} M C_7 and A_7 is < 3% the normalized abundance of the C_7^{2-} monomer (Figure 1b). The mixed dimer $A_7{\cdot}C_7^{3-}$ is less than 1% of the normalized abundance. It is possible to obtain dissociation spectra even for such low abundance ions by extensive signal averaging (vide infra).

Dissociation Pathways of Double Strand DNA.

The dissociation kinetics of seven triply charged duplexes with varying degrees of complementarity were measured over a temperature range of 55 to 210 °C ($(TGCA)_2^{3-}$, $(CCGG)_2^{3-}$, $(AATTAAT)_2^{3-}$, $(CCGGCCG)_2^{3-}$, $A_7{\cdot}T_7^{3-}$, $A_7{\cdot}A_7^{3-}$, and $T_7{\cdot}T_7^{3-}$). A representative BIRD spectrum of each of these duplexes taken from the kinetic data is shown in Figure 2. The Arrhenius activation energy (E_a) and preexponential factor (A) are obtained from an Arrhenius plot (Figure 3).

Complementary Duplexes.

The three duplexes which are composed of fully complementary strands, $(TGCA)_2^{3-}$, $A_7{\cdot}T_7^{3-}$, and $(CCGG)_2^{3-}$ (Figure 2a,b,g), dissociate almost exclusively to the corresponding single strands. For $A_7{\cdot}T_7^{3-}$, a small amount (~10%) of neutral adenine loss is observed at the lower temperatures, but this does not occur at higher temperatures.

The two monomers formed by dissociation of the duplex are formed in equal abundance. Their combined charge is equal to the original charge of the duplex. For example,

$(TGCA)_2^{3-}$dissociates to form equal amounts of $TGCA^{2-}$ and $TGCA^{-}$. The measured abundance ratio for these ions, $(TGCA)^{2-}$/ $(TGCA)^{-}$, is 3.0 to 1. The corresponding ratios for $A_7{\cdot}T_7^{3-}$ and $T_7{\cdot}T_7^{3-}$ are 1.8 and 3.8, respectively. The ion signal in FTMS is directly proportional to charge. Thus, a doubly charged ion should have twice the intensity of a singly charged ion. The higher ratio observed here could either be due to subsequent dissociation of the singly charged ion to produce lower mass fragment ions that are not observed due to poor signal-to-noise (S/N) or it could be due to high mass discrimination either by poor detection efficiency or by preferential ion loss at higher *m*/*z*. We have previously shown that correcting for an even larger *m*/*z* detection bias has an effect on the measured rate constant but changes the Arrhenius activation energy by less than 3%.[43] The E_a is the primary value of interest in this study. Therefore, no correction for mass discrimination was made to these data.

The Arrhenius parameters measured for dissociation of the three duplexes into the corresponding single strands are listed in Table 1. All three dissociation processes exhibit high preexponential factors, 10^{18}–10^{19} s^{-1}, consistent with the highly entropically favored cleavage of noncovalent bonds. The measured dissociation activation energies are 1.4 eV ($TGCA_2^{3-}$), 1.5 eV ($CCGG_2^{3-}$), and 1.7 eV ($A_7{\cdot}T_7^{3-}$).

It is interesting to note that dissociation of $A_7{\cdot}T_7^{3-}$ leads to a single charge state for each of the strands, T_7^{2-} and A_7^{-}, rather than a distribution. This indicates that the T_7^{-} strand has a lower apparent acidity (lower $\Delta G_{\mathrm{acid}}^{\mathrm{app}}$) than the A_7^{-} strand. BIRD of the negatively charged proton bound nucleic acid dimer, $A{\cdot}T^{-}$, results in charge retention exclusively by the thymine nucleic acid. This result indicates that the thymine nucleobase is better able to stabilize the deprotonated phosphate group, leading to a lower intrinsic acidity (lower ΔG_{acid}) for the T nucleotide residues compared with the A residues.

Partially Complementary Duplexes.

BIRD of the duplexes composed of partially self-complementary strands, $(AATTAAT)_2^{3-}$ and $(CCGGCCG)_2^{3-}$, does not lead predominantly to the individual strands. In both cases, extensive backbone fragmentation occurs leading to (**a** – base) and **w** type ions (nomenclature of McLuckey and co-workers[51]). The (**a** – base) and **w** ions, which are sequence specific, are produced by cleavage of the 3′ phosphoester bonds. The general structure of these ions is illustrated in Scheme 2. Dissociation of $(AATTAAT)_2^{3-}$ leads to the formation of some singly and doubly charged single strands, along with abundant loss of adenine and minor abundance of singly charged w_1, w_2, and (a_2 – AH) ions. The (**a** – base) and **w** type ions are formed by cleavage at sites adjacent to adenine residues. The propensity for cleavage adjacent to adenine residues has been observed for single-strand DNA.[52–54] The complementary fragments to these ions are not observed presumably due to their low abundance and possible subsequent dissociation via multiple pathways. However, this has the same effect on the measured kinetics as the detection problem discussed earlier. This does not significantly affect the measured E_a.43 Dissociation of the $(CCGGCCG)_2^{3-}$ dimer results in the formation of singly charged (a_2 – CH) to (a_5 – CH) and w_1 to w_5 fragment ions; no single strands are observed at any of the temperatures studied.

To determine how the (**a** – base) and **w** ions are formed from these duplexes, double resonance experiments were carried out for both $(AATTAAT)_2^{3-}$ and $(CCGGCCG)_2^{3-}$. In a double-resonance experiment, a single frequency rf excitation is applied for the duration of the BIRD reaction delay. This results in continuous ejection of a selected fragment ion from the cell thereby preventing subsequent dissociation of this ion from contributing to the BIRD spectrum.[44] Continuous ejection of the monomers during the dissociation of the duplexes did not result in a decrease of the abundance of the (**a** – base) and **w** ions. This indicates that the (**a** – base) and **w** fragment ions originate from the duplex and not from secondary dissociation processes

involving the single strands. Continuous ejection of the ion corresponding to duplex minus base results in nearly complete elimination of the (**a** – base) and **w** ions. This indicates that loss of a neutral base precedes backbone cleavage, as is observed with dissociation of single strands.[51,55] No complementary fragments to the (**a** – base) and **w** ions are observed, i.e., $(M_2 - 3H - \mathbf{a} - \text{base})^{2-}$ and $(M_2 - 3H - \mathbf{w})^{2-}$. Thus, backbone fragmentation resulting in the formation of (**a** – base) and **w** ions from one strand leads to the dissociation of the remaining noncovalent complex. The reason for this is not known.

The Arrhenius parameters for dissociation of $(AATTAAT)_2^{3-}$ by two competing processes, base loss and dissociation to single strands (Scheme 3), were obtained by extracting the individual rate constants, k_{bl} (base loss) and k_{ss} (dissociation to single strands), for the two parallel processes (Scheme 3) determined from the relative abundances of their respective product ions. These values are given in Table 1. The E_a and A for the formation of the single strands is 1.4 eV and 10^{16} s^{-1}, respectively. The E_a for base loss is 1.2 eV with a preexponential of 10^{13} s^{-1}. For $(CCGGCCG)_2^{3-}$, the Arrhenius parameters for base loss (CH and GH) is 1.5 eV and 10^{15} s^{-1}. Since no single strands are observed under these conditions, the E_a for dissociation of $(CCGGCCG)_2^{3-}$ into monomers cannot be measured. However, a lower limit to the E_a for this process can be obtained. The average A factor for dissociation into single strands for the four 7-mer duplexes which undergo this process is $10^{16.5}$ s^{-1}. This value is larger than that for base loss from $(CCGGCCG)_2^{3-}$, i.e., dissociation into single strands in entropically more favorable. Thus, the E_a for this process must be greater than 1.5 eV. A better estimate of this activation energy can be obtained by assuming that the A factor for this process is $10^{16.5}$ s^{-1}. If, at the highest temperature used, k_{ss} is less than 10% of k_{bl}, then the E_a for dissociation to monomers must be greater than 1.65 eV.

Noncomplementary Duplexes.

BIRD of the noncomplementary dimer, $A_7 \cdot A_7^{3-}$, results in substantial loss of neutral adenine and secondary (**a** – base) and **w** ions at longer times, as well as dissociation to the two monomers (Figure 2e). $A_7 \cdot C_7^{3-}$ also predominantly undergoes loss of neutral adenine (> 55%) (spectrum not shown). The $T_7 \cdot T_7^{3-}$ dimer dissociates exclusively to the two single strands (Figure 2f). The absence of base loss is consistent with our observation that neither T_7^{2-} nor T_7^{3-} dissociate at 220 °C, the highest temperatures presently attainable with our instrument. The Arrhenius parameters measured for $A_7 \cdot A_7^{3-}$ and $T_7 \cdot T_7^{3-}$ are listed in Table 1. Arrhenius parameters for $A_7 \cdot C_7^{3-}$ could not be obtained due to its low abundance in the ESI spectrum (Figure 2b). The E_a for dissociation to single strands was similar for both dimers, ~1.4 eV. Dissociation of $T_7 \cdot T_7^{3-}$ occurs with a higher preexponential factor, 10^{17} s^{-1}, compared to 10^{15} s^{-1} for $A_7 \cdot A_7^{3-}$, although, due to magnitude of the error limits, this difference may not indicate significant differences in the dissociation mechanism.

Discussion

Evidence for Watson–Crick Base Pairing in the Gas Phase.

The higher abundance of complementary versus non-complementary duplexes in an ESI mass spectrum does not signify that any structural specificity is retained in the gas-phase complexes. Removal of solvent must clearly influence the structure of these gas-phase ions. For example, charge groups that are surrounded by water in solution, interact with polarizable groups of the ion in the gas phase.[56–58] This can result in local distortions in structure near charge sites. However, some interactions, such as hydrogen bonding and van der Waals interactions, which are important in the solution-phase structure, are also expected to play a significant role in the gas phase. From gas-phase dissociation measurements as well as from modeling, we present four pieces of evidence which indicates that WC base pairing can survive the electrospray process and the removal of solvent.

i. E_a for Complementary versus Noncomplementary Duplexes.—The E_a for dissociation into single strands for $A_7{\cdot}A_7^{3-}$ (1.39 ± 0.15 eV) and $T_7{\cdot}T_7^{3-}$ (1.40 ± 0.08 eV) are the same within experimental error. In contrast, the E_a for $A_7{\cdot}T_7^{3-}$ (1.68 ± 0.11 eV) is significantly higher. If, upon removal of solvent, the three duplexes rearranged to random structures driven by gas-phase interactions, such as charge solvation, then the E_a of $A_7{\cdot}T_7^{3-}$ should be intermediate between $A_7{\cdot}A_7^{3-}$ and $T_7{\cdot}T_7^{3-}$. The higher E_a for $A_7{\cdot}T_7^{3-}$ indicates that the nature of the bases within *both* strands affects the strength of the interaction. We believe that the higher E_a for $A_7{\cdot}T_7^{3-}$ is due to the retention of the WC hydrogen bonds between the complementary bases. We see no other obvious reason for this higher E_a. It is important to note that the presence of WC base pairing in the gas phase does not necessarily imply that the three-dimensional structure of the double helix is maintained. As is illustrated by molecular modeling results, base pairing is possible in the absence of the double helix structure (vide infra).

ii. Attenuation of Base Loss in Complementary Duplexes.—Base loss represents a dominant dissociation pathway for all of the adenine containing 7-mer duplexes except for $A_7{\cdot}T_7^{3-}$. For this ion, base loss is observed only at lower temperatures and then only as a minor pathway. At ~120 °C, the rate constant for base loss from $A_7{\cdot}A_7^{3-}$ is equal to the rate constant for dissociation of $A_7{\cdot}T_7^{3-}$ into the individual strands. If the Arrhenius parameters for base loss were the same for these two dimers, then the ion corresponding to loss of adenine should have constituted ~50% of the observed fragment ion abundance in the $A_7{\cdot}T_7^{3-}$ spectrum. However, base loss from $A_7{\cdot}T_7^{3-}$makes up only ~10% of the normalized fragment ion abundance. Thus, the Arrhenius parameters for this fragmentation pathway are different for the two dimers. This difference cannot be due simply to the fact that $A_7{\cdot}A_7^{3-}$ contains twice as many adenine nucleobases; $A_7{\cdot}C_7^{3-}$ also dissociates predominantly by loss of neutral adenine (> 55%; no single strands are observed within the S/N). This indicates that the chemical environment of the bases and the ionized phosphate groups in the complementary versus noncomplementary dimers are different. We attribute the decreased lability of the adenine bases in $A_7{\cdot}T_7^{3-}$ to the bases being constrained or "locked into place" by WC base pairing. This increased solvation of the bases should lead to a higher E_a since cleavage of both the covalent and noncovalent bonds is required in order for the reaction to proceed. It should also be noted that the small amount of base loss that is observed for $A_7{\cdot}T_7^{3-}$ may be due to the presence of some dimers where the strands are shifted by one or more bases leading to unpaired bases and more facile loss of adenine due to this unpairing. The difference in ΔG_d in solution between the fully complementary pair $A_7{\cdot}T_7$ and the dimer that is shifted by one base, i.e., seven versus six Watson–Crick base pairs, is calculated to be only 2.0 kcal/mol.[50,59] Thus, some fraction of the duplexes in solution are likely to be shifted by one base. Evidence for enhanced base loss adjacent to a dangling end in non fully complementary duplexes is presented below.

iii. Solution versus Gas-Phase Dissociation Energetics.—Figure 4 shows the gas-phase E_a for dissociation of duplex to monomer versus the enthalpies (ΔH_d) for dimerization in solution for the five duplexes that are capable of WC base pairing.

$$M_2(aq) = 2M(aq) \quad (\Delta H_d)$$

The solution-phase enthalpies are calculated using the widely employed nearest-neighbor model[50] derived from solution thermochemistry measured for a series of oligonucleotide duplexes.[59] In this model, the thermochemical values for the dimerization of a given pair of oligonucleotides are determined from parametrized nearest neighbor contributions, plus an initiation term. This model has been demonstrated to reproduce experimentally determined dimerization enthalpies ($-\Delta H_d$) for a large number of 8–20-mer duplexes.[59] Included in this plot is the estimated lower limit for the dissociation of $(CCGGCCG)_2^{3-}$.

Within this limited data set, there appears to be a correlation between the calculated solution enthalpies and the measured gas-phase E_a values (correlation coefficient of 0.94). Clearly, additional and more accurate measurements are required to show more meaningful similarities or differences between the values. To the extent that a correlation does exist between the solution and gas-phase values, it indicates that the same interactions that stabilize the duplex in solution are also present in the absence of solvent, although the relative magnitude of these interactions may differ. The measured energetics for the noncomplementary dimers are not included in Figure 4. We are not aware of reliable solution-phase enthalpies for the noncomplementary DNA dimers.

iv. Molecular Modeling.—The triply charged dimers, $A_7{\cdot}T_7^{3-}$, $A_7{\cdot}A_7^{3-}$, and $T_7{\cdot}T_7^{3}$, were modeled by molecular dynamics using the Amber94 force field. This force field most accurately reproduces ab initio H-bonding and base stacking stabilization energies.[48,49] A double-helix structure was selected as the initial geometry in all three cases. Dynamics simulations were carried out for the three duplexes at 300 K. After 100 ps, the 14 WC hydrogen bonds initially present in $A_7{\cdot}T_7^{3-}$ remain intact (Figure 5a). Despite the conservation of base pairing, part of the helical structure is lost. The collapse of the helix appears to be the result of solvation of the deprotonated phosphate oxygen in the middle of the T_7 strand which interacts with an adjacent base within the same strand. The two terminal deprotonated phosphates are solvated by adjacent phosphate groups on the same strand. These results suggest that the double-helix structure may be more stable for the lower charge state ions. By examining the dissociation activation energies of duplexes as a function of charge state, information about how electrostatic interactions influence the stability of the duplexes could be obtained.

Molecular dynamics of the noncomplementary dimers at the same temperature (300 K) shows that the helical structures collapse within ~40 ps, with the dimers adopting a relatively compact structure. At ~100 ps, the two strands in the $A_7{\cdot}A_7^{3-}$ dimer are held together by an average of about eight hydrogen bonds between bases, as well as those between bases and the backbone (Figure 5b). Extensive intrastrand hydrogen bonding is also observed. A similar result is obtained for the $T_7{\cdot}T_7^{3-}$ dimer which also adopts a compact, ball-like structure (Figure 5c). On average, ~13 interstrand hydrogen bonds are present. For $A_7{\cdot}T_7^{3-}$, there are 14 WC hydrogen bonds between the strands. The slightly higher number of hydrogen bonds for $A_7{\cdot}T_7^{3-}$ versus the homodimers by itself does not explain the significantly higher E_a for this duplex. The hydrogen-bonding geometry in the $A_7{\cdot}T_7^{3-}$ duplex may be more favorable resulting in stronger hydrogen bonds.

To test the stability of the $A_7{\cdot}T_7^{3-}$ structure shown in Figure 5a, dynamics for this complex were continued for another 300 ps at 400 K (Figure 6). Even at this higher temperature and longer time, six of the seven WC base pairs remain intact. The terminal, unpaired bases (indicated by an asterisk) are found to participate in both inter- and intrastrand hydrogen bonding. The preservation of the majority of the WC base pairs at both 300 and 400 K supports the experimental data which indicates that WC pairing can be preserved in the gas phase.

Regioselective Dissociation.

An unexpected result in the present work is that base loss from the duplexes, $(AATTAAT)_2^{3-}$ and $(CCGGCCG)_2^{3-}$, is kinetically favored over base loss from the corresponding single strands. If WC base paired, these duplexes will have unpaired bases at both ends (Scheme 4). Figure 7 shows the BIRD spectra of both single-strand $(AATTAAT)^{2-}$ and double-strand $(AATTAAT)_2^{3-}$ at 124 °C with a dissociation delay of 105 s. Dissociation of the duplex results in base loss, formation of individual strands, and formation of (**a** – base) and **w** ions. Virtually no fragmentation is observed for either the doubly charged or the singly charged (data not shown) single strand under these same conditions. Data for the

triply charged single strand was not obtained due to its low abundance in the ESI spectrum. However, triply charged monomers were not observed in the dissociation spectra of any of the triply charged dimers. Thus, the (**a** -base) and **w** ions must originate from the duplex and not from the single strand. The (**a** – base) and **w** ions correspond to cleavage of the backbone bonds at the ends of the duplex, specifically at the terminal Watson–Crick base pairs. Enhanced dissociation at these same sites is also observed for the $(CCGGCCG)_2^{3-}$ dimer (Figure 8). Under the conditions used for the CCGGCCG ions, extensive dissociation of the single strand occurs but the abundance of both the w_1 and (a_2 – CH) ions is significantly larger in the dissociation of the duplex. Dissociation of the oligonucleotide backbone at the terminal Watson–Crick base pair does not occur for any of the fully complementary duplexes, although some base loss (10%) is observed for $A_7{\cdot}T_7^{3-}$ where some small fraction of the duplex is likely to be shifted (vide infra). This indicates that the dangling nucleobase is promoting base loss and/or subsequent cleavage at this site.

Base loss from both these duplexes occurs with a higher E_a and A factor than for the corresponding single strand. The E_a and A factor for base loss from $(AATTAAT)_2^{3-}$ are 1.2 eV and 10^{13} s^{-1}, while for the single-strand $AATTAAT^{2-}$, these values are 1.0 eV and 10^{10} s^{-1}. Similarly, values of 1.5 eV and 10^{15} s^{-1} are obtained for $(CCGGCCG)_2^{3-}$, in contrast to 1.3 eV and 10^{13} s^{-1} measured for $CCGGCCG^{2-}$. The net effect of these increased Arrhenius parameters is to reduce the thermal stability of the duplexes toward base loss relative to the corresponding single strand. Because of the enhanced formation of fragment ions from the terminal residues (Figures 7 and 8), these cleavages appear to be both regioselective and "catalytic." The driving force behind this catalytic activity in the gas phase is higher entropy. The bases, if WC base paired, are physically constrained in the dimer. Base loss would increase the conformational entropy in the transition state resulting in an entropically favored dissociation.

The ability to enhance backbone fragmentation at specific sites through complexation raises the interesting possibility of carrying out site-specific cleavage by complexing DNA with oligonucleotide primers that bind at specific sequence regions. Results of Griffey and Creig indicate that enhanced cleavage at sites of mismatch in duplexes occurs in collisionally activated dissociation.[60] Work is currently underway to evaluate the nature of the enhanced dissociation and strategies for use in DNA analysis.

Lifetimes of DNA 7-mer Duplexes in the Gas Phase.

The gas-phase dissociation activation energies of these DNA duplexes are quite high compared to dissociation of many covalent bonds in peptides, proteins, and DNA single strands.[43,44,46,61] From the Arrhenius parameters in the present work, it is possible to calculate rate constants at lower temperatures. For example, from the E_a and A values measured for the dissociation of $T_7{\cdot}T_7^{3-}$ to single strands, the rate constant at standard temperature (298 K) would be 2.7×10^{-7} s^{-1}. This corresponds to a half-life of ~30 days! The only assumption in extrapolating rate constants to lower temperatures is that the E_a and A values measured at higher temperature correspond to the lowest energy process. This is likely to be true for the $T_7{\cdot}T_7^{3-}$ ion since neither base loss nor backbone fragmentation is observed for the single- or double-strand ions at higher temperatures and the A factor for formation of monomers is large.

For $A_7{\cdot}T_7^{3-}$, the rate constant at standard temperature (298 K) determined using the Arrhenius parameters measured at 118–149 °C is 6.2×10^{-10} s^{-1}. This corresponds to a half-life of ~35 years! This half-life is an upper limit because a parallel reaction (base loss) is observed in the BIRD spectra at the lower temperatures. The absence of this process at higher temperatures indicates that loss of base occurs with both a lower E_a and A factor than does dissociation to the single strands. Consequently, one would anticipate a larger rate constant at standard temperature for base loss compared to dissociation to the monomers. Ions can be thermalized

within several seconds in the FTMS cell. These results indicate that the lifetimes of these noncovalent DNA complexes in the gas phase will not present an impediment to any practical experiment. In addition, these results clearly demonstrate that solvent is not necessary to stabilize double-strand DNA in the gas phase.

Conclusions

The Arrhenius activation energies and preexponential factors for the dissociation of seven triply charged duplexes with varying degrees of complementarity have been measured using BIRD. These are the first quantitative measurements of DNA dissociation energetics in the gas phase. Dissociation of the duplexes results in cleavage of the noncovalent interactions to produce the monomer ions and/or cleavage of covalent bonds resulting in base loss and subsequent formation of sequence-specific (**a** – base) and **w** ions.

Four independent pieces of evidence are presented which indicate that WC base pairing can be preserved into the gas phase. No one piece of evidence considered individually provides a compelling case. However, when considered together, these pieces provide strong support for the existence of gas-phase Watson–Crick base pairing. These pieces of evidence are the following: i. the dissociation activation energy of the complementary duplex, $A_7{\cdot}T_7^{3-}$, is higher than that of the two related noncomplementary dimers, $A_7{\cdot}A_7^{3-}$ and $T_7{\cdot}T_7^{3-}$, indicating that the nature of the bases in both strands affects the strength of the interstrand binding, ii. molecular modeling results show that WC base pairs are stable in the case of $A_7{\cdot}T_7^{3-}$, while the noncomplementary dimers, $A_7{\cdot}A_7^{3-}$ and $T_7{\cdot}T_7^{3-}$, adopt a random structure with fewer interstrand hydrogen bonds, iii. loss of neutral adenine is a dominant dissociation pathway for all of the adenine-containing 7-mer duplexes with the exception of $A_7{\cdot}T_7^{3-}$ where this dissociation process is effectively shut down (this is attributed to greater solvation of the bases, consistent with the conservation of WC base pairing), iv. a correlation is observed between the gas-phase dissociation activation energies and the dimerization enthalpies in solution. This correlation indicates that not only WC base pairing, but other interactions that are present in solution, such as base stacking, may play a role in the gas-phase stability and structure of these complexes. Clearly, additional measurements are required to further elucidate the role of WC base pairing, base stacking, and electrostatic interactions on DNA duplex structure and stability in the gas phase. Nevertheless, we believe that the results presented here provide strong evidence that WC base pairing can exist in the complete absence of solvent.

Acknowledgements

The authors are grateful to Dr. Neil Kelleher for helpful discussions and providing sample micro-electrospray tips, Dr. Ted Thannhauser for synthesis and purification of the DNA samples, and Mr. Luis Comolli for aid with the measurement of DNA melting curves. This research would not have been possible if not for the generous financial support provided by the National Science Foundation (CHE-9258178 and CHE-9726183), National Institutes of Health (1R29GM50336-01A2), the Society of Analytical Chemists of Pittsburgh for sponsoring fellowship support though the American Chemical Society, Division of Analytical Chemistry (P.D.S.), and the Canadian NSERC for fellowship support (J.S.K).

References

1. Fenn JB, Mann M, Meng CK, Wong SF, Whitehouse CM. Science 1989;246:64–71. [PubMed: 2675315]
2. Hillenkamp F, Karas M, Beavis RC, Chait BT. Anal Chem 1991;63:1193A–1202A. [PubMed: 1897719]
3. Bowers MT, Marshall AG, McLafferty FW. J Phys Chem 1996;100:12897–12910.
4. a McLafferty FW. Acc Chem Res 1994;27:379–386.and references therein. b Kelleher NL, Senko MW, Siegel MM, McLafferty FW. J Am Soc Mass Spectrom 1997;8:380–383.

5. Cody RB Jr, Amster IJ, McLafferty FW. Proc Natl Acad Sci USA 1985;82:6367–6370. [PubMed: 2413438]
6. Hunt DF, Yates JR, Shabanowitz J, Winston S, Hauer CR. Proc Natl Acad Sci USA 1986;83:6233–6237. [PubMed: 3462691]
7. Dongre AR, Somogyi A, Wysocki VH. J Mass Spectrom 1996;31:339–350. [PubMed: 8799282]
8. Little DP, Chorush RA, Speir JP, Senko MW, Kelleher NL, McLafferty FW. J Am Chem Soc 1994;116:4893–4897.
9. Little DP, McLafferty FW. J Am Chem Soc 1995;117:6783–6784.
10. Nordhoff E, Kirpekar F, Roepstorff P. Mass Spec Rev 1996;15:67–138.
11. McLuckey SA, Habibigoudarzi S. J Am Chem Soc 1993;115:12085–12095.
12. Przybylski M, Glocker MD. Angew Chem 1996;35:807–826.and references therein.
13. Smith RD, Light-Wahl KJ. Biol Mass Spectrom 1993;22:493–501.
14. Smith DL, Zhang ZQ. Mass Spectrom Rev 1994;13:411–429.
15. Lim HK, Hsieh YL, Ganem B, Henion JD. J Mass Spectrom 1995;30:708–714.
16. Siuzdak G, Krebs JF, Benkovic SJ, Dyson HJ. J Am Chem Soc 1994;116:7937–7938.
17. Ganem B, Li YT, Henion JD. J Am Chem Soc 1991;113:7818–7819.
18. Ganem B, Li YT, Henion JD. J Am Chem Soc 1991;113:6294–6296.
19. Bayer E, Bauer T, Schmeer K, Bleicher K, Maier M, Gaus H. Anal Chem 1994;66:3858–3863. [PubMed: 7810895]
20. Doktycz MJ, Habibigoudarzi S, McLuckey SA. Anal Chem 1994;66:3416–3422. [PubMed: 7978315]
21. Ding J, Anderegg RJ. J Am Soc Mass Spectrom 1995;6:159–164.
22. Aaserud DJ, Kelleher NL, Little DP, McLafferty FW. J Am Soc Mass Spectrom 1996;7:1266–1269.
23. Greig MJ, Gaus HJ, Griffey RH. Rapid Commun Mass Spectrom 1996;10:47–50. [PubMed: 8563016]
24. Ganem B, Li YT, Henion JD. Tetrahedron Lett 1993;34:1445–1448.
25. Wolynes P. Proc Natl Acad Sci USA 1995;92:2426–2427. [PubMed: 7708658]
26. Hunter CL, Mauk AG, Douglas DJ. Biochemistry 1997;36:1018–1025. [PubMed: 9033391]
27. Gross DS, Zhao Y, Williams ER. J Am Soc Mass Spectrom 1997;8:519–524. [PubMed: 16479269]
28. Wu Q, Jinming G, Joseph-McCarthy D, Sigal GB, Bruce JE, Whitesides GM, Smith RD. J Am Chem Soc 1997;119:1157–1158.
29. Li YT, Hsieh YL, Henion JD, Senko MW, McLafferty FW, Ganem B. J Am Chem Soc 1993;115:8409–8413.
30. Sinden, R. R. DNA Structure and Function; Academic Press Inc.: New York, 1994.
31. Goodlett DR, Camp DG III, Hardin CC, Corregan M, Smith RD. Biol Mass Spectrom 1993;22:181–183. [PubMed: 8461341]
32. Greig MJ, Gaus H, Cummins LL, Sasmor H, Griffey RH. J Am Chem Soc 1995;117:10765–10766.
33. Gale DC, Goodlett DR, Light-Wahl KJ, Smith RD. J Am Chem Soc 1994;116:6027–6028.
34. Iannitti P, Sheil MM, Wickham G. J Am Chem Soc 1997;119:1490–1491.
35. Price WD, Schnier PD, Jockusch RA, Strittmatter EF, Williams ER. J Am Chem Soc 1996;118:10640–10644. [PubMed: 16467929]
36. Price WD, Williams ER. J Phys Chem A 1997;101:8844–8852. [PubMed: 16604162]
37. Dunbar RC, McMahon TB, Tholmann D, Tonner DS, Salahub DR, Wei D. J Am Chem Soc 1995;117:12819–12825.
38. Lin CY, Dunbar RC. J Phys Chem 1996;100:655–659.
39. Price WD, Schnier PD, Williams ER. J Phys Chem B 1997;101:664–673. [PubMed: 17235378]
40. Gross DS, Williams ER. Int J Mass Spectrom Ion Process 1996;158:305–318. [PubMed: 16479265]
41. Price WD, Jockusch RA, Williams ER. J Am Chem Soc 1997;119:11988–11989. [PubMed: 16479267]
42. Sena M, Riveros JM. J Phys Chem 1997;101:4384–4391.
43. Schnier PD, Price WD, Jockusch RA, Williams ER. J Am Chem Soc 1996;118:7178–7189. [PubMed: 16525512]

44. Schnier PD, Price WD, Strittmatter EF, Williams ER. J Am Soc Mass Spectrom 1997;8:771–780. [PubMed: 16554908]
45. Price WD, Schnier PD, Williams ER. Anal Chem 1996;68:859–866.
46. Jockusch RA, Schnier PD, Price WD, Strittmatter EF, Demirev PA, Williams ER. Anal Chem 1997;69:1119–1126. [PubMed: 9075403]
47. Cornell WD, Cieplak P, Bayly CI, Gould IR, Mertz KM, Ferguson DM, Spellmeyer DC, Fox T, Caldwell JW, Kollman PA. J Am Chem Soc 1995;117:5179–5197.
48. Šponer J, Leszczynski J, Hobza P. J Biomol Struct Dyn 1996;14:117–133. [PubMed: 8877568]
49. Hobza P, Kabelác M, Šponer J, Mejzlik P, Vonprasek J. J Comput Chem 1997;18:1136–1150.
50. Saenger, W. Principles of Nucleic Acid Structure; Springer-Verlag: New York, 1984.
51. McLuckey SA, Van Berkel GJ, Glish GL. J Am Soc Mass Spectrom 1992;3:60–70.
52. Rodgers MT, Campbell S, Marzluff EM, Beauchamp JL. Int J Mass Spectrom Ion Process 1995;148:1–23.
53. Habibi-Goudarzi S, McLuckey SA. J Am Soc Mass Spectrom 1995;6:102–113.
54. McLuckey SA, Vaidyanathan G, Habibi-Goudarzi S. J Mass Spectrom 1995;30:1222–1229.
55. Marzluff EM, Campbell S, Rodgers MT, Beauchamp JL. J Am Chem Soc 1994;116:7787–7796.
56. a Gross DS, Williams ER. J Am Chem Soc 1995;117:883–890. b Gross DS, Williams ER. J Am Chem Soc 1996;118:202–204.
57. Wyttenbach T, von Helden G, Bowers MT. J Am Chem Soc 1996;118:8355–8364.
58. Rodriguez-Cruz SE, Klassen JS, Williams ER. J Am Soc Mass Spectrom 1997;8:565–568.
59. SantaLucia JJ, Allawai HT, Seneviratne A. Biochemistry 1996;35:3555–3562. [PubMed: 8639506]
60. Griffey, R. H.; Greig, M. J. Proceedings of the 45th ASMS Conference on Mass Spectrometry and Allied Topics; Palm Springs, California, June 1–5, 1997.
61. Klassen, J. S.; Schnier, P. D.; Williams, E. R. J. Am. Soc. Mass Spectrom. In press.

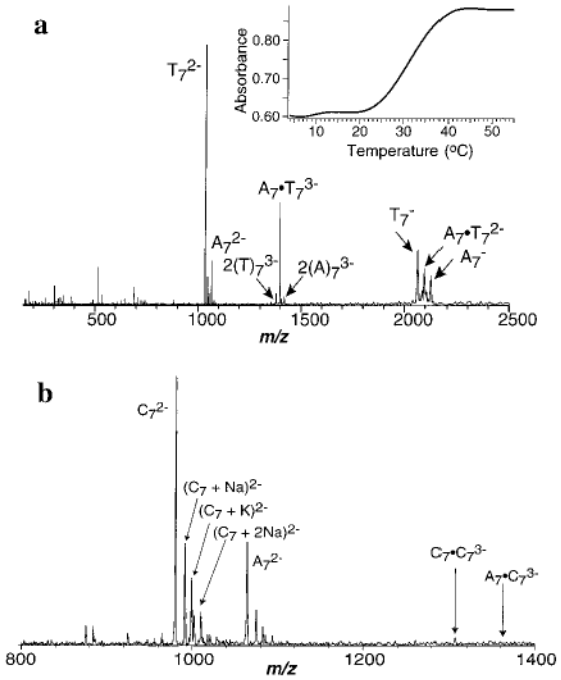

Figure 1.

Electrospray ionization Fourier transform mass spectra from 50:50 H_2O/CH_3CN solutions containing (a) 10^{-4} M $p(dA)_7$ and $p(dT)_7$ (inset shows the absorbance (260 nm) versus temperature profile (temperature melt) indicating the presence of double-helix DNA in this solution ($T_m \approx 32$ °C)) and (b) 10^{-4} M $p(dA)_7$ and $p(dC)_7$.

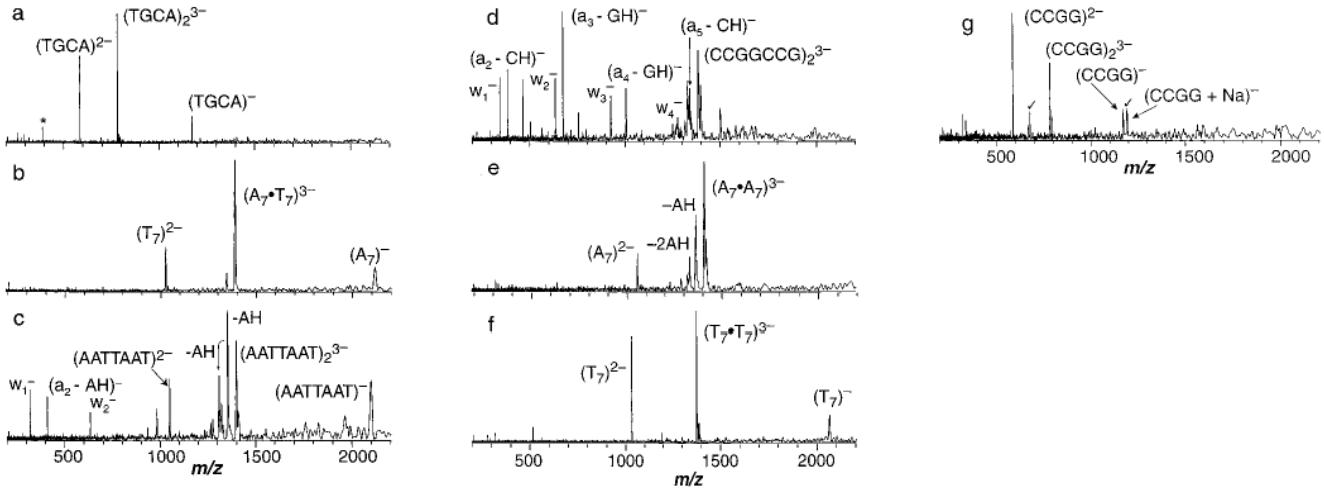

Figure 2.

Blackbody infrared radiative dissociation spectra of DNA duplexes with three negative charges taken from the kinetic data (a) $(TGCA)_2$, (300 s, 57 °C), (b) $A_7{\cdot}T_7$ (120 s, 117 °C), (c) $(AATTAAT)_2$ (45 s, 137 °C), (d) $(CCGGCCG)_2$ (150 s, 171 °C), (e) $A_7{\cdot}A_7$ (10 s, 150 °C), (f) $T_7{\cdot}T_7$ (20 s, 107 °C), and (g) $(CCGG)_2$ (30 s, 90 °C). An asterisk indicates a harmonic of the precursor ion. Checks indicate unejected ions; these ions do not interfere with the dissociation kinetics of interest. The spectrum shown in g was background subtracted.

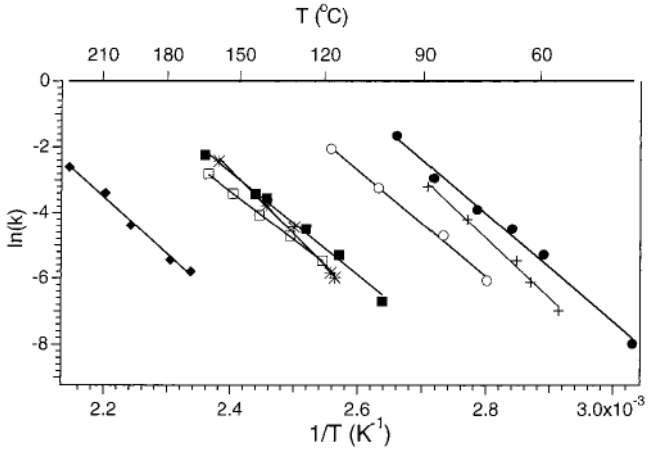

Figure 3.

Arrhenius plots for the dissociation of double-strand DNA (•) $(TGCA)_2^{3-}$, (○) $T_7{\cdot}T_7^{3-}$, (▪) $(AATTAAT)_2^{3-}$, (□) $A_7{\cdot}A_7^{3-}$, (*) $A_7{\cdot}T_7^{3-}$, (♦) $(CCGGCCG)_2^{3-}$, and (+) $(CCGG)_2^{3-}$.

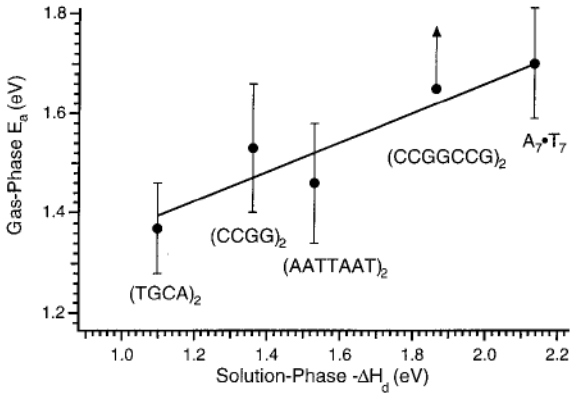

Figure 4.

Plot of calculated dimerization enthalpies ($-\Delta H_d$) for DNA duplexes in solution versus gas-phase activation energies for dissociation to monomer. The point for $(CCGGCCG)_2$ is a lower limit since no monomer is observed in the dissociation spectra (see text).

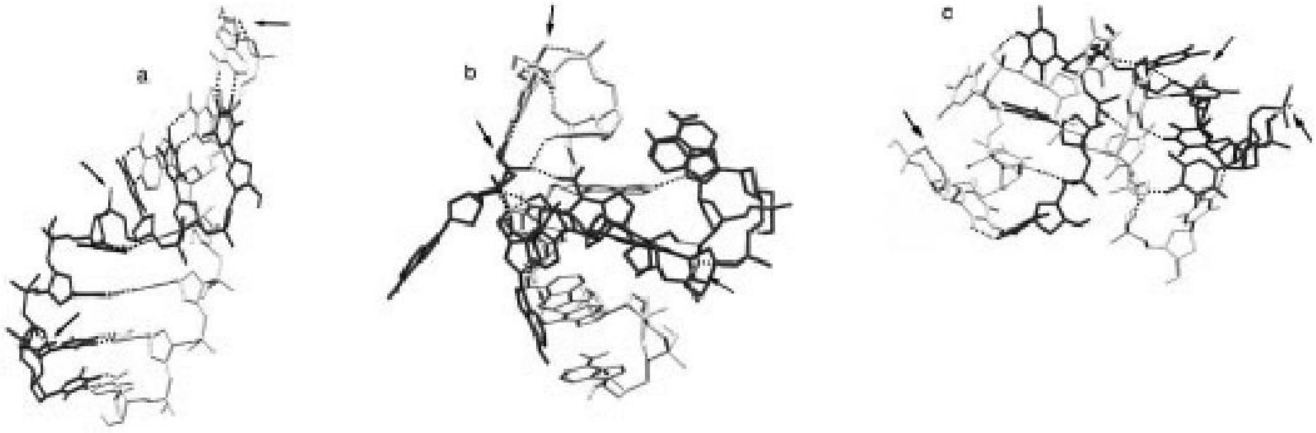

Figure 5.
Structure obtained from molecular dynamics simulations of $A_7 \cdot T_7^{3-}$, $A_7 \cdot A_7^{3-}$, and $T_7 \cdot T_7^{3-}$ after 100 ps at 300 K: (a) $A_7 \cdot T_7^{3-}$ (the dark strand corresponds to T_7), (b) $A_7 \cdot A_7^{3-}$, and (c) $T_7 \cdot T_7^{3-}$. Hydrogen bonds are indicated by dashed lines. Location of the charge sites are indicated by the arrows. Hydrogen atoms not involved in hydrogen bonding are omitted for clarity.

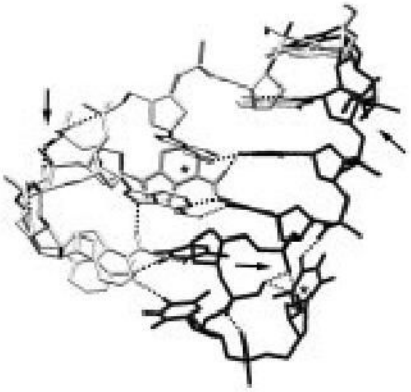

Figure 6.
Structure of $A_7 \cdot T_7^{3-}$ obtained by molecular dynamic simulations after 300 ps at 400 K. The structure in Figure 5a was used as the starting geometry (400 ps total simulation time). Six of the seven Watson–Crick base pairs remain; the two terminal unpaired bases are indicated by asterisks.

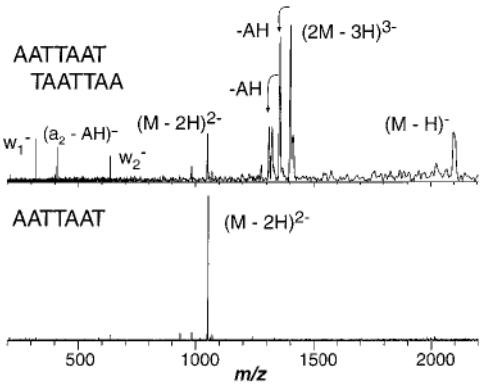

Figure 7.
BIRD spectra of (a) $(AATTAAT)_2^{3-}$ and (b) $AATTAAT^{2-}$ with a reaction delay of 105 s at 124 °C.

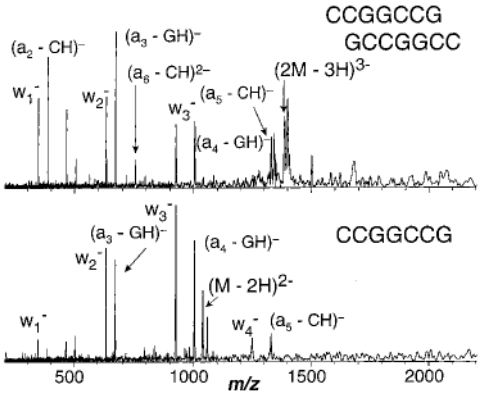

Figure 8.
BIRD spectra of (a) $(CCGGCCG)_2^{3-}$ and (b) $CCGGCCG^{2-}$ with a reaction delay of 90 s at 181 °C.

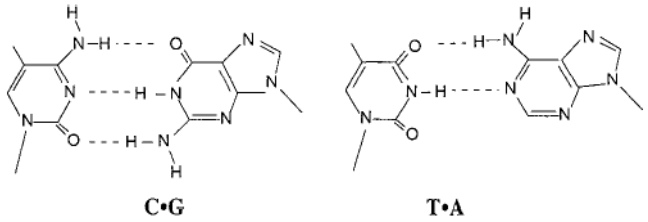

Scheme 1.

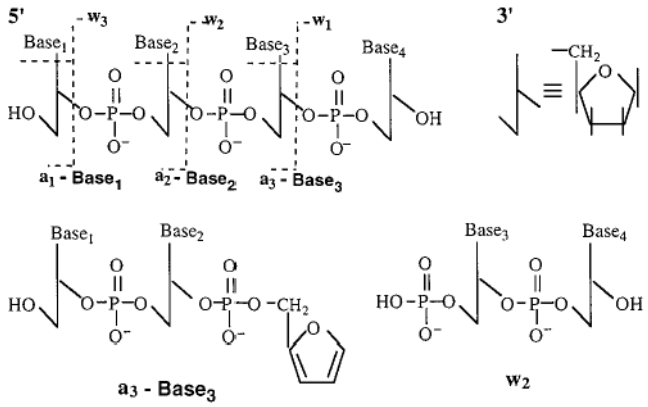

Scheme 2.

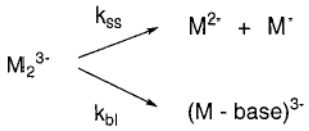

Scheme 3.

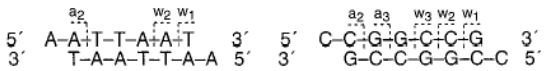

Scheme 4.

Table 1

Measured Arrhenius Activation Parameters for Dissociation of Double-Strand DNA Anions

oligonucleotide	activation energy (eV)	log (frequency factor)	primary fragments
$(TGCA)_2^{3-}$	1.41 ± 0.09	18.2 ± 1.3	monomer
$(CCGG)_2^{3-}$	1.51 ± 0.13	19.7 ± 1.6	monomer
$(AATTAAT)_2^{3-}$			-AH, monomer
overall	1.35 ± 0.08	15.1 ± 1.0	
→ monomer	1.44 ± 0.12	15.5 ± 1.2	
→ -AH	1.19 ± 0.08	13.0 ± 0.9	
$(CCGGCCG)_2^{3-}$			w_1 to w_4, (a_2 – CH) to (a_5 – CH)
overall	1.51 ± 0.11	15.2 ± 1.3	
→ monomer	(>1.65)[a]	(16.5)	
$A_7 \cdot C_7^{3-}$			-AH
$A_7 \cdot A_7^{3-}$			-AH, monomer
overall	1.26 ± 0.03	13.8 ± 0.2	
→ monomer	1.39 ± 0.15	14.8 ± 1.2	
→ -AH	1.22 ± 0.02	13.2 ± 0.4	
$T_7 \cdot T_7^{3-}$	1.40 ± 0.08	17.1 ± 1.1	monomer
$A_7 \cdot A_7^{3-}$	1.68 ± 0.11	19.2 ± 1.4	momomer, -AH (<10%)

[a] Value is an estimated lower limit (see text).